International Journal of Pharmacology

ISSN 1811-7775

science alert

ansinet
Asian Network for Scientific Information

OPEN ACCESS International Journal of Pharmacology

ISSN 1811-7775
DOI: 10.3923/ijp.2020.351.366

Research Article
Chlorpheniramine Maleate Induced Cardiotoxicity, Hepatotoxicity and Antioxidant Gene Expression Changes in Male Wistar Rats

[1,5]Sherifa S. Hamed, [1]Sherine Abdel Salam, [2,3]Manal F. El-Khadragy, [2]Wafa A. AL-Megrin, [4]Zeinab K. Hassan and [5]Esraa M. Shuker

[1]Department of Zoology, Faculty of Science, Alexandria University, Alexandria, Egypt
[2]Biology Department, Faculty of Science, Princess Nourah Bint Abdulrahman University, Riyadh, Saudi Arabia
[3]Department of Zoology and Entomology, Faculty of Science, Helwan University, Cairo, Egypt
[4]Department of Cancer, National Cancer Institute, Cairo University, Cairo, Egypt
[5]Department of Zoology, College of Science, King Saud University, Riyadh, Saudi Arabia

Abstract

Background and Objective: Chlorpheniramine maleate (CPM), an H1-receptor antagonist, belongs to the first generation of antihistamines. It is used in the treatment of allergy and has several adverse effects. The main purpose of this study is to evaluate the possible adverse effects of chlorpheniramine maleate on major target organs: Heart, liver and blood in young male Wistar rats. **Materials and Methods:** One dose was used, 2 mg kg^{-1} b.wt., with 2 different times of duration; the first treated group of the animal was given the former dose of CPM orally twice a day for 5 successive days. The second treated group of animals was given 2 mg kg^{-1} b.wt., of CPM orally twice a day for 5 successive days; then animals were rest left for one week after which the oral CPM at dose level 2 mg kg^{-1} b.wt., was administered twice for another 5 successive days. **Results:** CPM produced changes in the treated groups. Histopathological and cytopathological changes were recorded in the hepatocytes and cardiac muscle fibers of all treated groups with CPM. The effect of CPM on the activity of the mRNA of antioxidant genes was detected by using semi-quantitative RT-PCR. The expression of catalase (CAT), glutathione peroxidase (GSHPx) and glutathione-S-transferase (GST) in the liver, heart and blood were altered compared to the control. **Conclusion:** The current study demonstrated that chlorpheniramine maleate has cardiotoxic and hepatotoxic effects by increasing the free radical formation and decreasing the ability of the internal antioxidant defense system to detoxify reactive oxygen species.

Key words: Chlorpheniramine maleate, liver, heart, ultrastructure, antioxidant genes, liver markers

Citation: Sherifa S. Hamed, Sherine Abdel Salam, Manal F. El-Khadragy, Wafa A. AL-Megrin, Zeinab K. Hassan and Esraa M. Shuker, 2020. Chlorpheniramine maleate induced cardiotoxicity, hepatotoxicity and antioxidant gene expression changes in male wistar rats. Int. J. Pharmacol., 16: 351-366.

Corresponding Author: Sherifa S. Hamed, Department of Zoology, Faculty of Science, Alexandria University, Alexandria, Egypt

Competing Interest: The authors have declared that no competing interest exists.

Data Availability: All relevant data are within the paper and its supporting information files.

INTRODUCTION

Allergy is a major health problem in most modern societies[1] , with a high prevalence of certain allergic diseases in industrialized countries worldwide. Allergy prevalence was estimated to range between 10-40% according to the World Allergy Organization (WAO) report issued in 2013. It affects more than 20% of populations of most developing countries[2,3].

Antihistamines are widely used in human and veterinary medicine for relief from allergic diseases[4]. They are classified into 2 categories, classical (first generation) and second-generation agents. Classical antihistamines have a sedating effect leading to car accidents as well as accidents at work which affect productivity drastically. These effects are due to penetration through the blood-brain barrier and the occupation of brain histamine H1-receptors in the histaminergic neuron system[5,6].

One of the most commonly used antihistamines is Chlorpheniramine maleate (CPM), an H1-receptor antagonist, belongs to the first generation of antihistamine. It is considered as an important contributing factor in blocking histamine that the body makes during an allergic reaction. CPM is extensively used in the treatment and alleviating many kinds of allergy.

Generally, antihistamines are among the most commonly prescribed medicines in pediatrics. Opioids are also among the common drugs for cough and cold. The FDA updated the safety labeling of these medications, including Tussionex® Pennkinetic® and decided to restrict their uptake to patients ranged from $\geq$18 years, stating "these products will no longer be indicated for use to treat cough in any pediatric population" (FDA 2)[3] .

One of the main causes of the limited use of these drugs is that most of the antihistamines undergo liver transformation to metabolites that may or may not be active and whose concentrations in plasma depend on the activity of the P450 enzyme system[7].

Among them, CPM has been reported to produce a variety of adverse effects such as sedation, which can range from slight drowsiness to deep sleep[8]. Other side effects include rapid or irregular heartbeat, which interacts with some neurotransmitters and receptors of cardiac muscle, hypotension, liver problems including jaundice. CPM is also reported to produce numerous effects on major body systems such as sedation and other CNS effects in school children[9].

Toxicity has been reported to be a major reason accountable for the attrition of ~1/3 of drug candidates and a fundamental participant to the high cost of drug development, especially when not identified till the clinical trials or at the post-marketing phase[10].

On the other hand, detoxification is a pivotal metabolic process that protects living organisms against such harmful effects. The glutathione transferases (formerly known as glutathione S-transferases, GSTs) are one of the detoxification key players across many phyla and species[11]. Similarly, glutathione peroxidase (GPx) is a well-known Se-containing enzyme that has a vital role in cell defense against toxicity, oxidative stress and the conservation of intracellular redox environment[12].

Eventually, the noteworthy antioxidant enzyme, Catalase, has an important function in cell defense against oxidative damage of H_2O_2 through its dismutation into oxygen and water without consummation of endogenous reducing equivalents[13]. Thus, owing to the widespread use of antihistamines as a therapy of allergy, this investigation aimed to evaluate the adverse effects of CPM on the heart and liver by using, light and electron microscopes bioassays in young male Wistar rats. Some antioxidant gene expression profiles were analyzed to evaluate these effects.

MATERIALS AND METHODS

Animals: Forty young healthy, 15 days old laboratory male Wistar rats weighing about 110-140 g were obtained from animal house King Saud University. The animals were housed in plastic cages under controlled temperature (23±28°C) and maintained in groups of ten per cage in a natural light-dark cycle. They were given free access to a commercial pellet diet and tap water and allowed to acclimatize for 3 days before initiation of the experiment. All experimental procedures involving animals were conducted in accordance with the guidelines of the National Program for Science and Technology of Faculty of Science, King Saud University during the period from January, 2016-September, 2017. The study protocol was approved (No. 1/3/12149) by Ethical Committee of King Saud University (KSU), Riyadh.

Drug used: Chlorpheniramine maleate ($C1_6H1_9ClN_2{\cdot}C_4H_4O_4$) syrup (Histop) is manufactured by SPIMACO company, purchased from Saudi Pharmaceutical Industries and Medical Appliances Corporation (Saudi Arabia).

Experimental groups: The experimental animals were divided into four groups, each consist of 10 rats. The dose of chlorpheniramine maleate used in the present study was equivalent to the pediatric therapeutic doses[14]:

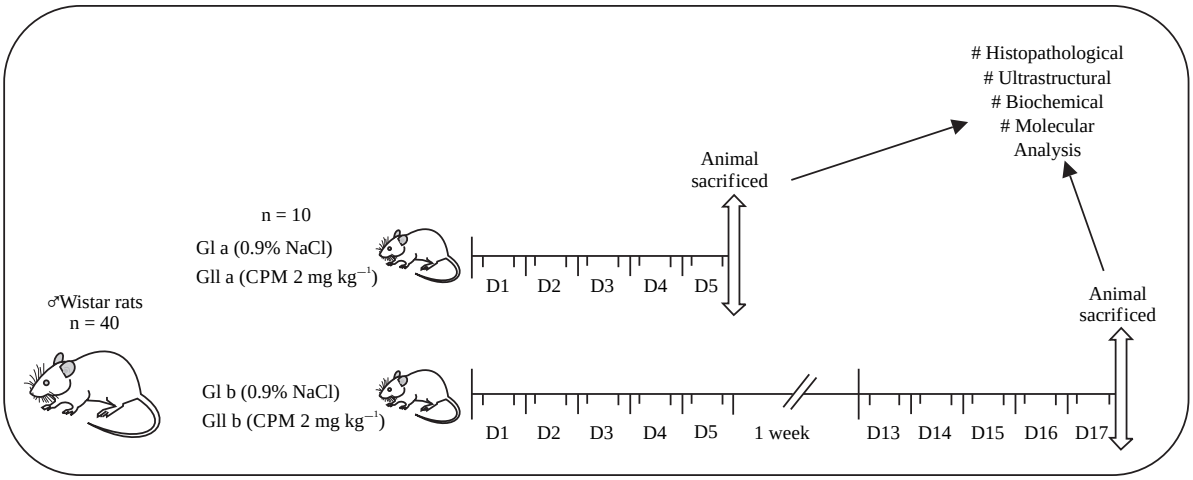

Fig. S1: Timeline for experimental procedure

GI: Control group which was divided into 2 groups:

- **GI a:** The animal was given orally 0.045 mL normal saline (0.9% NaCl) twice a day for 5 successive days, i.e., the animal received 0.45 mg kg^{-1} b.wt., cumulative dose
- **GI b:** The animals were given orally 0.045 mL normal saline (0.9% NaCl) twice a day for five successive days, animals were rest left for 1 week after which the above dose was repeated for another 5 successive days, i.e., the animal received 0.9 mL kg^{-1} b.wt., cumulative dose

GII: Animals were divided into two groups:

- **GII a:** The animals were given orally 0.045 mL CPM dose twice a day at dose level (2 mg^{-1} b.wt.) for 5 successive days, i.e., the animal received 0.45 mL kg^{-1} b.wt., cumulative dose
- **GII b:** The animals were given orally 0.045 mL CPM dose twice a day at a dose level (2 mg^{-1} b.wt.) for 5 successive days, animals were rest for 1 week after which the oral CPM at a dose level (2 mg^{-1} b.wt.) were administered for 5 successive days , i.e., the animal received 0.9 mL kg^{-1} b.wt., cumulative dose

The behavior, external features and the percentage of mortality in each group (control and treated groups) of the rat were recorded every day. Heart and liver of rats in each group were recorded and were weighed at the ending of the experiment (i.e. after 17 days) then the mean organ weight was calculated.

After 5 and 17 days of treatment, a definite number of rats from control and treated groups were randomly chosen. The timeline for the experimental procedure is represented in Fig. S1.

Supplementary material

Histopathological and ultrastructural studies: One hour after the last treatment, unanesthetized rats from both control and treated groups were sacrificed by decapitation. Small pieces from the apex of the heart and liver were immediately removed for light and transmission electron microscopes examinations.

Light microscopic studies: Specimens were fixed in 10% Neutral Buffered Formalin (NBF). The standard method of dehydration, clearing in xylene and paraffin embedding (melting point 56°C) was used and were cut at 5 µm thick by rotary microtome and were stained with hematoxylin and eosin[15].

Transmission electron microscopic studies: Specimens of GI b and GII b were fixed in 4% glutaraldehyde in phosphate buffer (pH 7.4), post-fixed in 2% osmium tetroxide (OsO_4), dehydrated in graded acetone and embedded in Epon. Sections were cut of 1 µm thick and were stained with Toluidine Blue (TB) for light microscopy. Thin sections were cut on ultra-microtome, place on grids, were double-stained with uranyl acetate and lead citrate and were examined with transmission electron microscope[16].

Bioassay studies: Rats from control and treated groups were anesthetized with ether. The blood samples were obtained

Table 1: Primers sequence for catalase (CAT), glutathione peroxidase (GSHPx) and glutathione-s-transferase (GST) genes used in semi-quantitative PCR

Gene name	Forward primer	Reverse primer
CAT	5'-AGG TGA CAC TAT AGA ATA GTG GTT TTC ACC GAC GAG AT-3'	5'-GTA CGA CTC ACT ATA GGG ACA CGA GGT CCC AGT TAC CAT-3'
GSHPx	5'-GGG CAA AGA AGA TTC CAG GTT-3'	5'-AGA GCG GGT GAG CCT TCT-3'
GST	5'-GCC TTC TAC CCG AAG ACA CCT T-3'	5'-GTC AGC CTG TTC CCT ACA-3'

from the retro-orbital sinus of the eye into no additive sterile tube (red top plain) and were centrifuged at 2500 rpm for 10 min. Sera were separated and were transferred to a labeled pour-off tube. Measurement and analysis of alanine transaminase (ALT) and alkaline phosphatase (ALP) were estimated by diagnostic kits purchased from United Diagnostics Industry UDi, KSA. ALT diagnostic kit (UDi) CAT. No. CB 07-750 and ALP diagnostic kit (UDi) CAT. No. CB 04L-750.

Biochemical and molecular studies: Immediately after blood samples were collected from the retro-orbital sinus of the eye into in (EDTA) tubes, animals were then sacrificed by decapitation after exposure to ether in desiccators and their livers and hearts were rapidly excised and kept immediately frozen at -80°C and used for determining the activity of antioxidant enzymes and markers of oxidative stress. Each sample was tested in triplicate.

cDNA synthesis and semi-quantitative RT-PCR methods: Total RNA was extracted from blood, liver and heart tissue by using isolation kit (AxyPrep Multisource Total RNA Miniprep Kit), according to the manufacturer's protocol. The RNA concentrations and quality were measured Nanodrop (NanoDropIno, Wilmington, DE, USA). The isolated RNA has an A 260/280 ratio of 1.9-2.1. According to the manufacturer, the first-strand cDNA was synthesized from 1 µg of total RNA by reverse transcription with a SuperScript TM first-strand synthesis system kit (Invitrogen, CA, USA). RT-PCR was done according to a previous study[17]. All primers[17] were listed in Table 1.

Statistical analysis: Liver and heart weights, measurements of nuclei, mitochondria and sarcomere, ALT and ALP serum levels are presented as Means±SE. The results were computed statistically using the SPSS software package. Significance of changes as a result of drug treatment was assessed using a one-way analysis of variance (ANOVA).

RESULTS

Mortality rate, behavior and external features of rats: An increase in food intake was recorded in animals treated with CPM. Sleepiness, indolence and inactivity were observed in treated rats (GII a and GII b groups). The percentage of mortality of rats among all groups (control and treated) was zero.

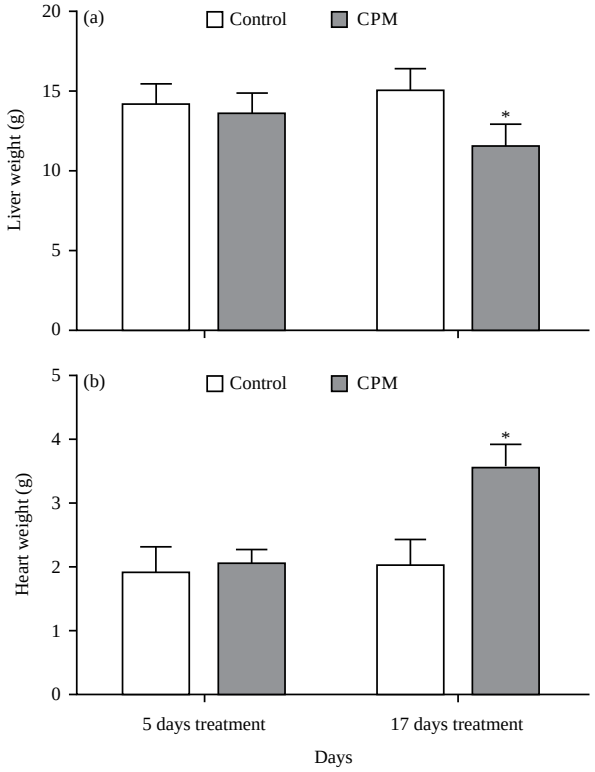

Fig. 1(a,b): Chlorpheniramine maleate (CPM) induced hepatotoxicity and cardiotoxicity in young male Wistar rats (a) Liver weight of GII b as compared to the control and (b) heart weight of GII b as compared to control GI b values are Means±SEM (n =10)

*p<0.05, vs. control (one-way analysis of variance (ANOVA) followed by Duncan's test)

Liver and heart weights: The liver of the control group was reddish-brown, soft and smooth, with an evident gloss. While in the two treated groups (GII a and GII b), abnormal liver with very soft and dark reddish-brown was observed. The weight changes of liver and heart of control and GII b were recorded after 17 days (at the end of the experiment) (Fig. 1). There was a significant decrease in the liver weight of GII b when compared to the control GI b group (Fig. 1a). However, a

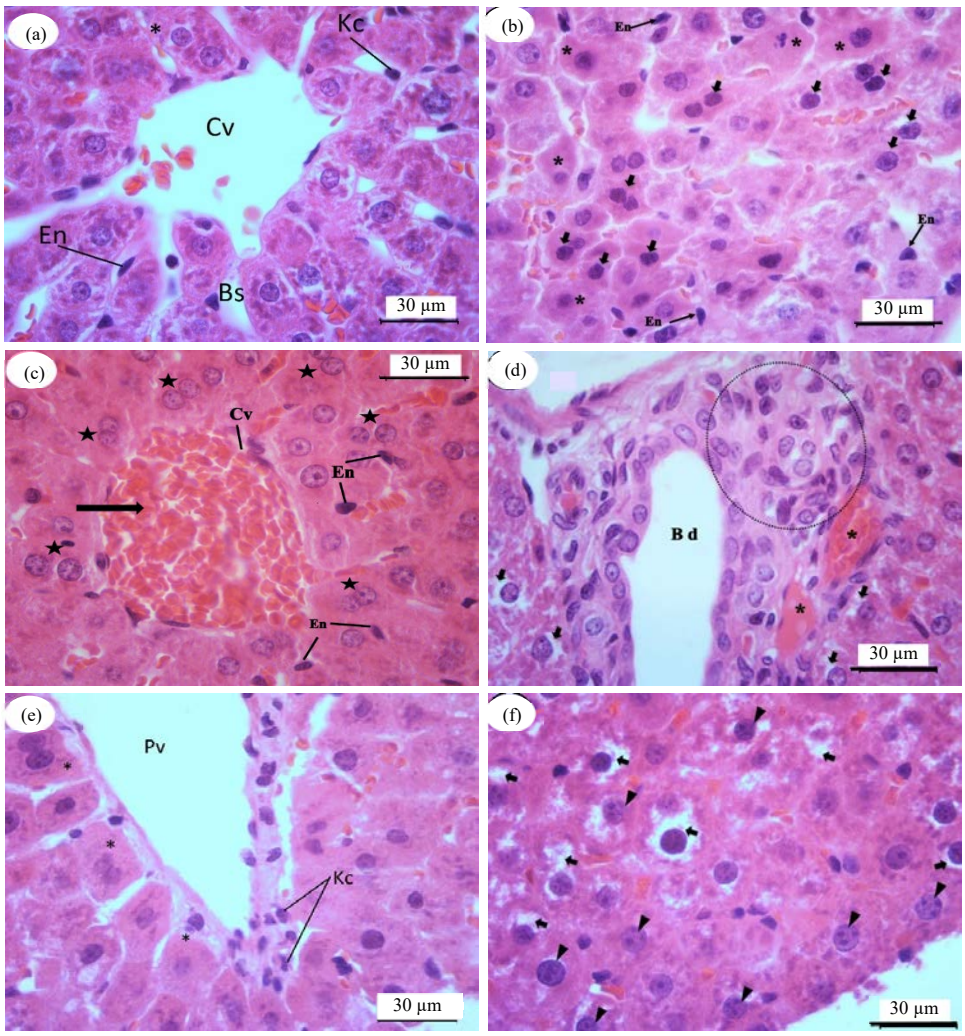

Fig. 2(a-f): Light micrographs of the liver of control (GI) and treated groups (GII a, b)

(a) Control (GI) showing hepatic plates separated by blood sinusoids (Bc), Endothelial cell (En), Kupffer cell (Kc), hepatocytes (asterisk)with finely granular cytoplasm ; and blood sinusoid (Bs) open into central vein (Cv). (b-f) Treated groups, (b) (GII a): Increase of pleomorphic pyknotic nuclei (arrow) and hyalinization of hepatocytes (asterisks), (c) (GII a): Normal architecture of the hepatic lobules was lost and congestion of central vein (Cv) which filled with RBCs stasis (arrow), hypertrophied endothelial (En) of sinusoids, hyalinization of hepatocytes and increase in the frequency of binucleated cells (stars), (d) (GII a):Vacuolated hepatocyte (arrows) , hemorrhage of sinusoids (asterisks), proliferated epithelium (circle) of bile duct (Bd), (e) (GII b): Kupffer cells (Kc) around the portal vein (Pv) and swelling of hepatocytes (asterisks), (f) (GII b): Hepatocytes with high vacuolation(arrows) and nuclei with multiple nucleoli (arrow head), (H and E), (scale bar 30 µm)

significant increase in the heart weight of GII b treated group compared to the control GI b (Fig. 1b).

Microscopic observations

Liver: All general aspects of liver were evident. It was surrounded by a thin layer of connective tissue sheath and the hepatic lobules are not delimited by a layer of connective tissue. Hepatic centrilobular veins, from which anastomosing plates or cords of parenchymal cells (hepatocytes) radiate and a system of irregular sinusoids were recognized. The conspicuous portal tract consisting of connective tissue, in which a branch of the hepatic portal vein, the hepatic artery, the bile duct and lymphatic vessel. The hepatic plates are composed of polyhedral hepatocytes and euchromatic nuclei centrally located, with one or more nucleoli. Frequently binucleated hepatocytes were shown (Fig. 2a).

In both treated groups GII a and GII b, the normal architecture of the hepatic lobules was lost (indistinct boundaries between the cells). Hypertrophied hepatocytes and an increase in the frequency of binucleated cells were observed (Fig. 2b) Hepatocytes with pleomorphic, pyknotic, karyorrhexis and karyolysis nuclei with irregular

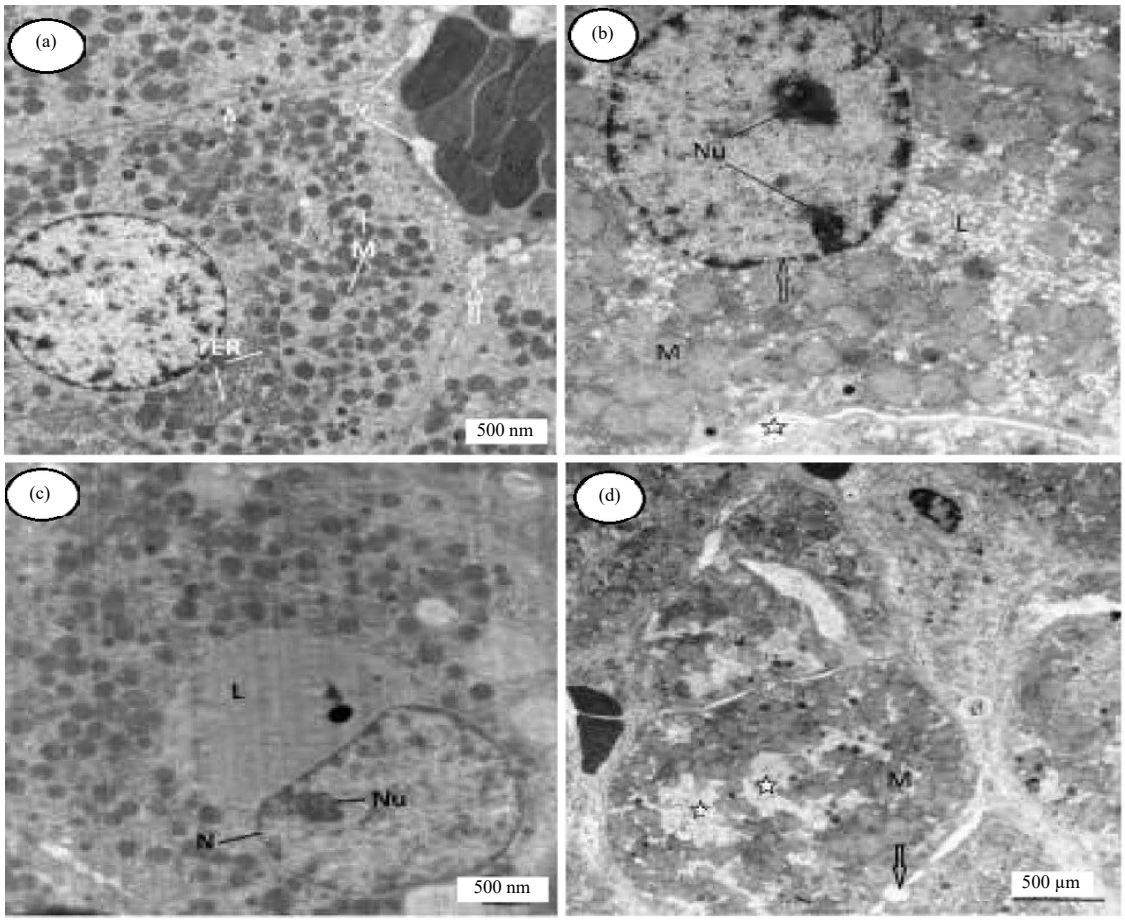

Fig. 3(a-d): Electron micrographs of the liver

(a) Shows hepatocytes in control rats with a polygonal outline and central round large nucleus and its cytoplasm was full with abundant round or ovoid mitochondria, rough endoplasmic reticulum (rER), lysosome and dense aggregates of glycogen, (b-d) Show hepatocytes in GII b treated rats, with the irregularity of nuclear envelope(arrow), (b) Peripheral nucleus (N), (c) Margination of the nucleolus (Nu) (b,c), wandered bile canaliculi (arrows) and lipid (star) (d) Severe fragmentation and aggregation of mitochondria (M)

nuclear envelope and hypereosinophilia were observed. Dilation, congestion and hypertrophied endothelium of blood sinusoids, hepatic central vein and hepatic portal vein were observed. Also, hepatic portal veins were filled with RBCs (stasis) (Fig. 2c). The ductal proliferation of biliary epithelium was observed as well as proliferated stromal cells (Fig. 2d). Moreover, increased and activated hypertrophied Kupffer cells being were pushed within the sinusoidal lumen (Fig. 2e). The hepatic portal vein zone was more seriously affected than the central vein. The cytoplasm of hepatocytes of GII b was highly vacuolated than GII a, in addition to the hyalinization of the cytoplasm (Fig. 2f). Indeed, the liver of rat treated with CPM showed that the pathological changes and their frequencies are increased with increasing time of exposure or (cumulative dose) i.e., GII b·GII a.

In the control rat, EM picture of hepatocytes appeared with a polygonal outline and central round large nucleus and its cytoplasm were full of abundant round or ovoid mitochondria, rough endoplasmic reticulum (rER), lysosome and dense aggregates of glycogen (Fig. 3a). However, in treated GII b, hepatocytes showed a peripheral nucleus with their regularity of nuclear envelope and margination of the nucleolus. Also, fragmentation of mitochondria and necrotic areas were seen. An increase of intercellular space as well as widened bile canaliculi was observed (Fig. 3b-d).

Heart: In the light microscope of the control rat, all general aspects of cardiac muscle fiber morphology were evident. Cardiac muscle fibers (cells) from the heart wall were striated, tubular and branched. Transverse lines that cross the chains of cardiac cells at the level of the Z-lines, the intercalated discs, represented the interface between adjacent muscle cells (Fig. 4a). However, in CPM treated groups (GII a and GII b), a scattered light patch of muscle fibers was observed due to

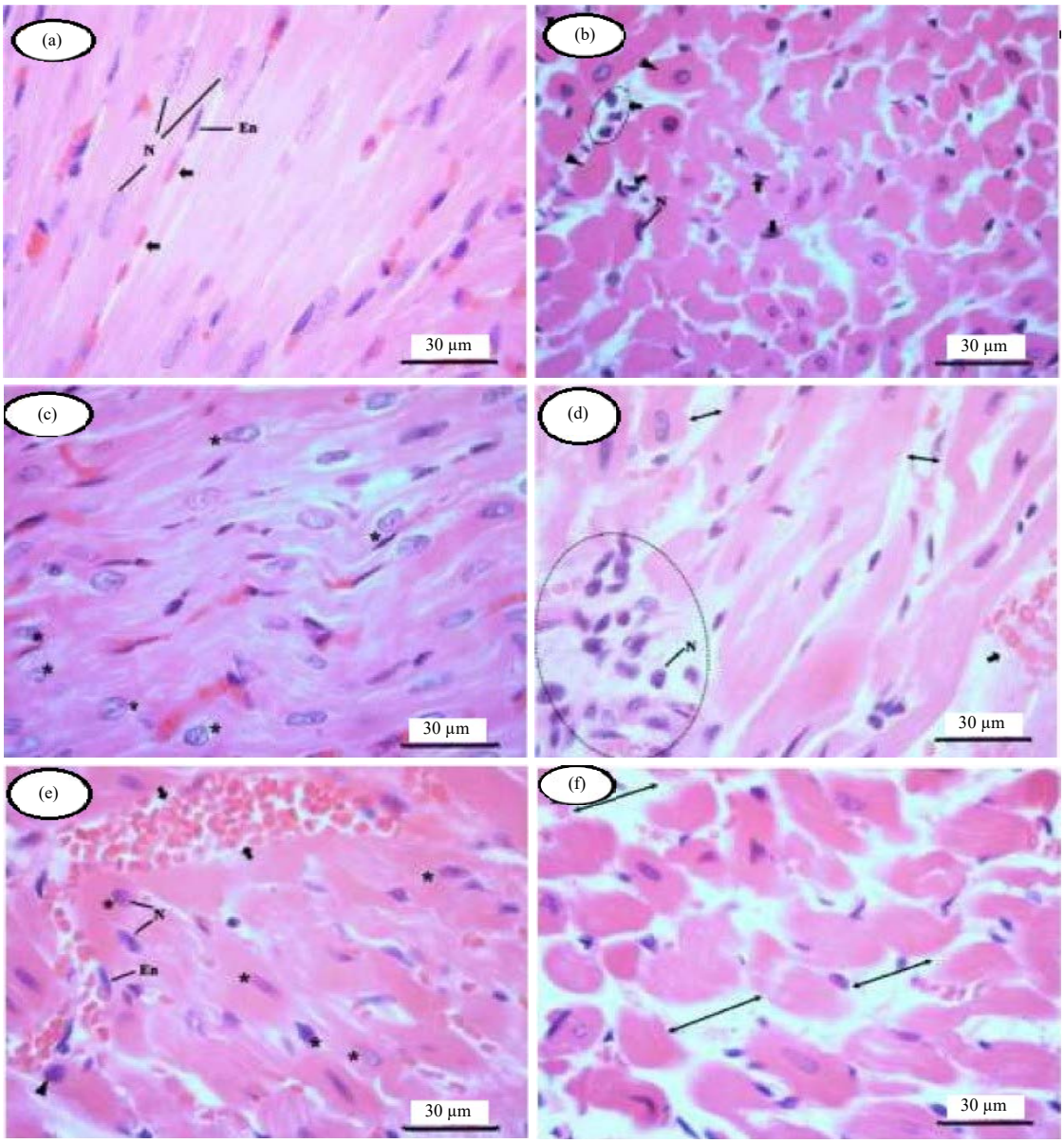

Fig. 4(a-f): Light micrographs of the cardiac muscle

(a) Shows the normal histological structure of cardiac muscle in the control group, (b) (GII a) shows deeply eosinophilic cytoplasm (head arrows) of cardiac muscle, pyknotic basophilic nuclei (N), slightly focal myofilament loss (asterisks) mononuclear cell infiltration (arrows), (c) (GII a): Cardiac muscle show a decrease of nuclear size (asterisks) as well as an increase of its basophilia; slightly wavy muscle fibers, (d) (GII a) Shows focal area of dissociated necrotic cell with an indistinct outline (circle); pyknotic nuclei (N); wide capillaries with RBCs stasis (arrow), abnormal spacing between muscle fiber (↔), (e) (GII b): Cardiac muscle with congestion of blood capillaries and RBCs stasis (arrows) lined with hypertrophied endothelial (En); polymorphic nuclei (head arrows); margination of nuclei (asterisks), (f) (GII b) Shows abnormal spacing between muscle bundles fibers (↔), Scale bar 30 µm

myofilaments loss (Fig. 4b). In addition the following was detected; a focal waving of muscle fibers (Fig. 4c) an increase of spacing between muscle bundles (Fig. 4d) proliferated widened capillaries with hypertrophied endothelial pyknotic nuclei; RBCs stasis (Fig. 4e) and marginated pleomorphic shrunken nuclei of cardiac muscle. Indeed, GII b was more affected (Fig.4f) than GII a.

In an electron microscope, the control group showed a typical EM structure of cardiac muscle (Fig. 5a), while in the treated group (GII b), a typical striation appeared side by side to abnormal striation myofibrils was observed than control (Fig. 5b). Disorganized cardiac myofibrils with indistinct light and dark bands of its sarcomeres (Fig. 5c) and pleomorphic, abnormal and fragmented mitochondria (Fig. 5d) were seen.

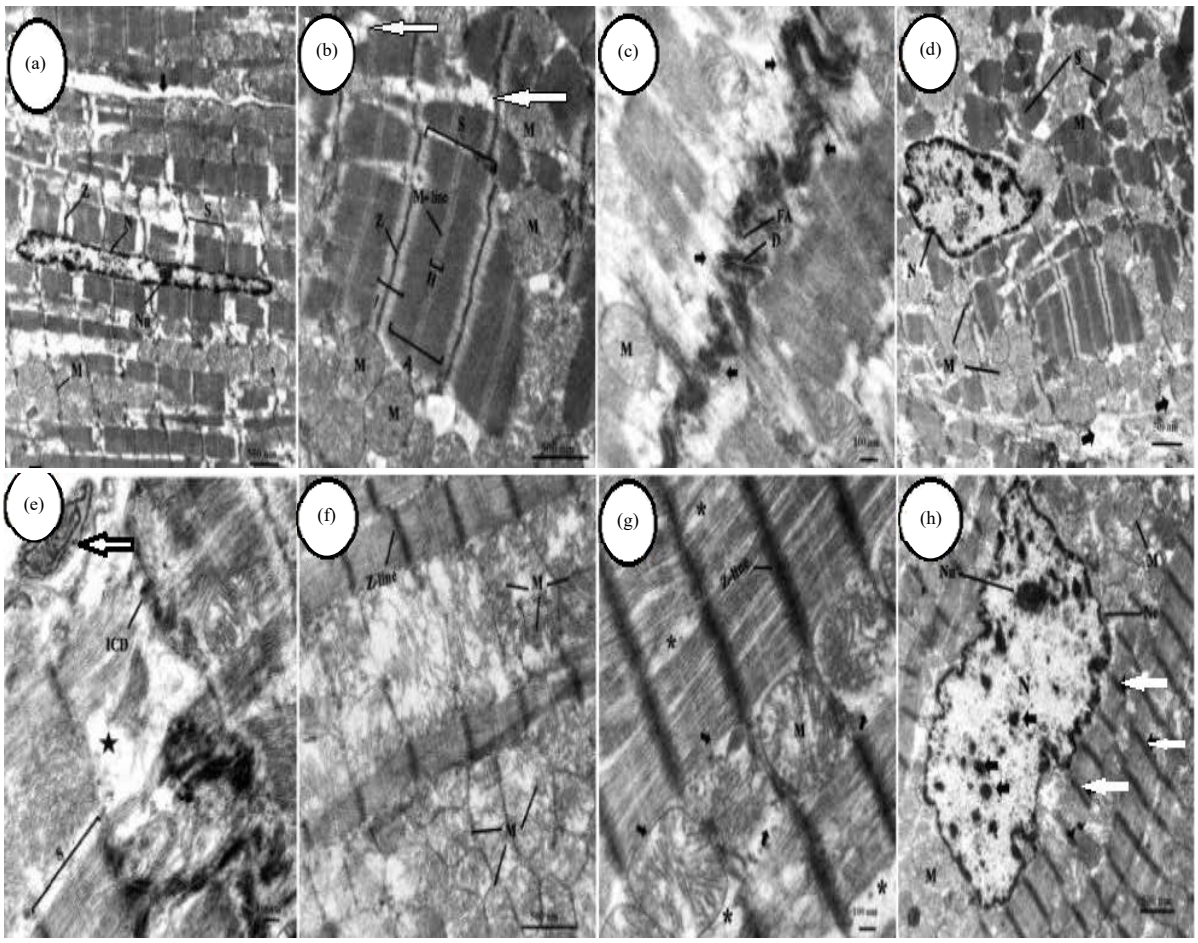

Fig. 5(a-h): Electron micrographs of cardiac muscle

(a) Control group showing nucleus (N) of cardiac muscle fiber with nucleolus (Nu), sarcomere(S), Z-line (Z), mitochondria (M), sarcoplasm (arrow); (b-h) show treated group (GII b), (b) Shows typical striation appeared side by side, sarcomere (S) to abnormal striation myofibrils (arrow). (c) Thickened Z-line appeared as well disrupted intercalated disc (arrows), Fascia Adherens (FA), Desmosomes (D), (d) Disorganized myofibrils with indistinct light and dark bands of its sarcomeres (s), ruptured sarcolemma (arrows), (e) Increase and decrease of sarcomere length (S), complete loss of sarcomere (star), indistinct intercalated disc (ICD), nerve ending (arrow), (f) Destructed cristae of mitochondria (M), (g) Indistinct light and dark bands (stars), disrupted mitochondrial membranes (arrows) (h) Hypertrophied bizzard shape nuleus (N) with undulated nuclear envelope (Ne) and marginated nucleolus (Nu), fragmented heterochromatin (black arrows), thickened Z-line (white arrows)

Disrupted intercalated discs were evident within myofibrils (Fig. 5e). Ruptured, lysed mitochondria with light vacuolized matrix, disrupted and destructed cristae, were observed near the sarcolemma (Fig. 5f). Moreover, a thickened Z-line was seen (Fig. 5g). CPM induced nuclei with abnormal outlines (bizzard shape), marinated heterochromatin and abnormally condensed nucleoli (Fig. 5h).

A significant decrease in length of the myocardial nuclei (Fig. 6a) and an insignificant increase in its nuclear width (Fig. 6b) of GII b as compared to the control were observed. GII showed a significant decrease in mitochondrial length of the myocardium (Fig. 6c) and an insignificant increase of mitochondrial width of myocardium than control (Fig. 6d). Also, a significant decrease in sarcomere length was observed than control (Fig. 6e).

Bioassay results: Liver Enzymes, ALT enzyme showed that in CPM-induced a non-significant change level than the control GI b and it was increased in group GII b compared to the control group. ALP enzymes showed that in CPM-induced a highly statistically significant increase in treated GII b compared to the control group (Fig.7 a and b).

Molecular data results: The effect of CPM on the mRNA expression of antioxidant genes *CAT*, *GSHPx* and *GST* in blood, liver and heart tissue was investigated by quantitative detection of the gene mRNA expression. In the blood, the *CAT* mRNA expression of GII (a and b groups) was significantly decreased compared to the control group (Fig. 8 a-c), however, *CAT* mRNA expression was significantly increased

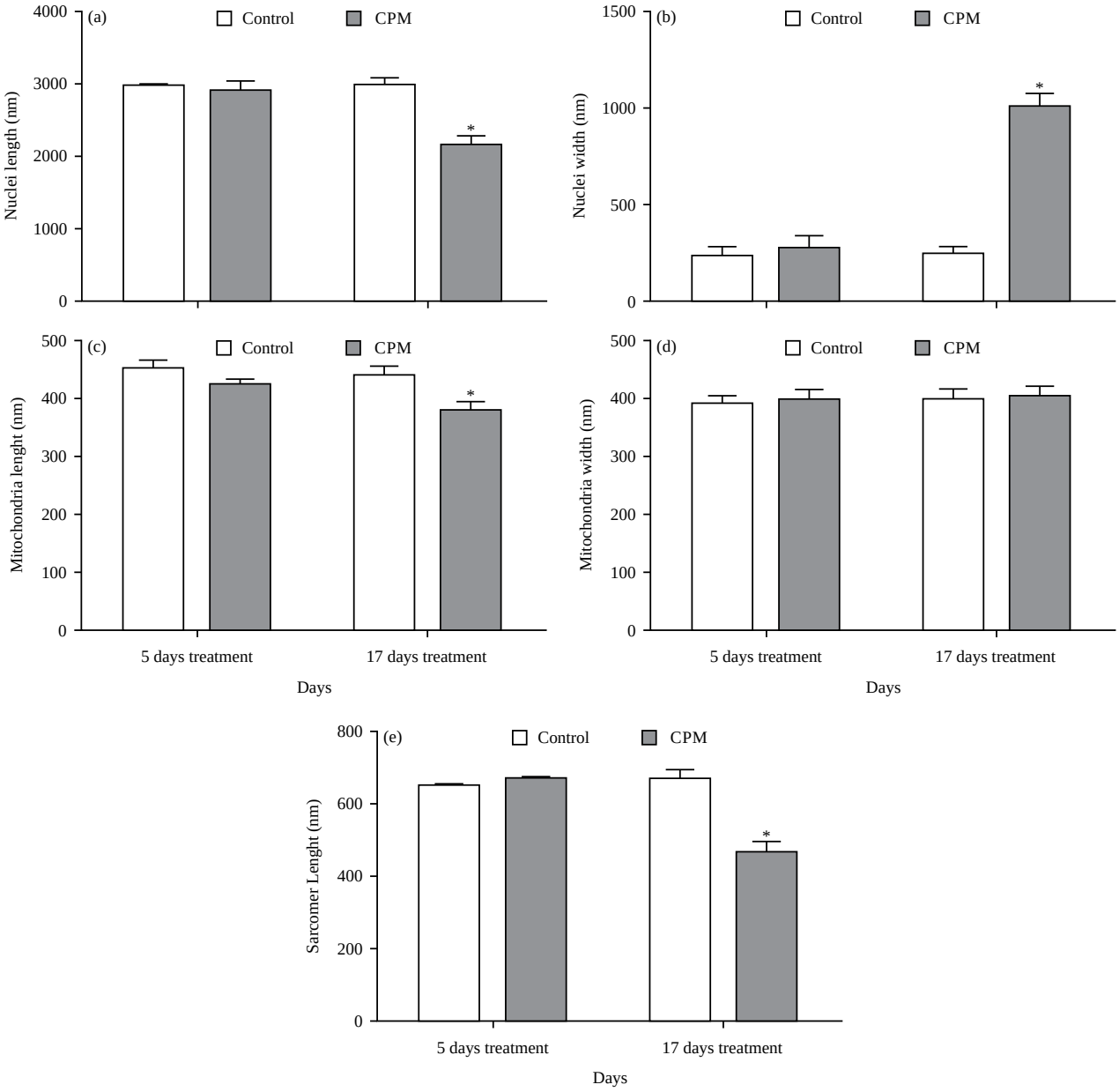

Fig. 6(a-e): CPM(GII b) induced a significant decrease in the length of myocardial (a) Nuclei than control, (b) A Significant increase in nuclear width of the myocardium as compared to the control, (c) Notice a significant decrease in mitochondrial length of myocardium and (d) Insignificant increase of mitochondrial width of myocardium of GII b than control, In addition, (e) There was a significant decrease in sarcomere length of GII b than control

Values are Mean±SEM (n = 10),*p<0.05, vs. Control (one-way analysis of variance (ANOVA) followed by Duncan's test)

compared to control in the liver and cardiac muscle. On the other hand, The *GSHPx* and *GST* mRNA expression regulation showed a significant down-regulation in all of the studied groups (Fig. 9 a-c and Fig. 10 a-c).

The main findings of the present study are summarized in Fig. 11.

DISCUSSION

CPM belongs to H1-antihistamines, with the following main side effects: (1) Depression of the CNS due to their poor receptor selectivity and high penetration rate of the blood-brain barrier, leading to drowsiness, fatigue,

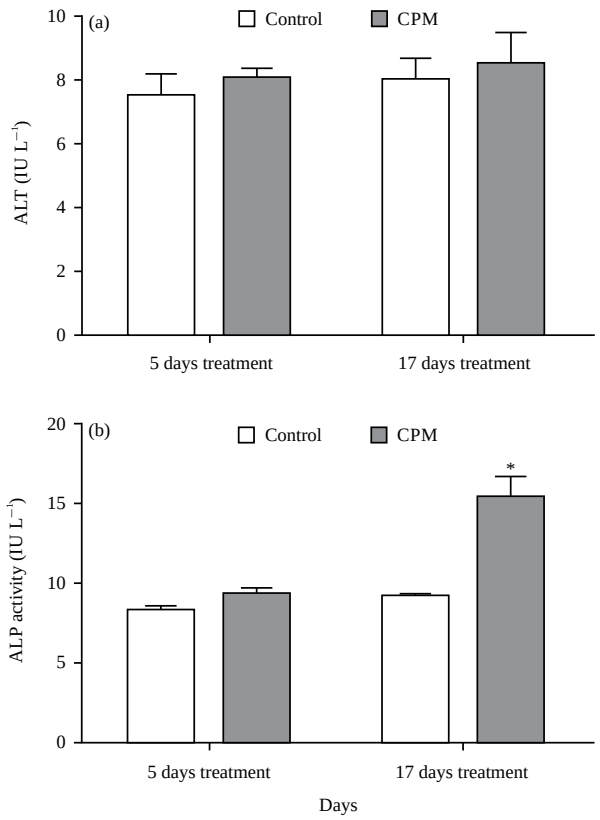

Fig. 7(a-b): Alanine transaminase (ALT) and alkaline phosphatase (ALP) level in CPM-induced toxicity in young male Wistar rats

Values are mean±SEM (n = 10),*p<0.05, vs. control (one-way analysis of variance (ANOVA) followed by Duncan's test)

somnolence and dizziness, as well as impairments of cognitive function, memory and psychomotor performance, (2) Cardiac problems (cardiotoxicity) due to antimuscarinic effects, α-adrenergic–receptor blockade and blockade of cardiac ion currents and (3) Other problems due to blockade of muscarinic, α-adrenergic and serotonergic receptors, leading to mydriasis, dry eyes, dry mouth, urinary retention, gastrointestinal motility, constipation, erectile dysfunction, memory deficits[18] and have also been associated with fatalities in accidental and intentional pediatric overdose[19,20].

The action of histamine is mainly mediated by H1-receptor. The role of histamine and H1-receptor during development was also demonstrated in knockout mouse models, in which the loss of function of either H1-receptor or histidine decarboxylase (the histamine-producing enzyme) can cause brain function impairment such as; learning and memory, insomnia and pain perception[21].

In a knock out mouse model, the vital role of histaminergic neurons in maintaining wakefulness under

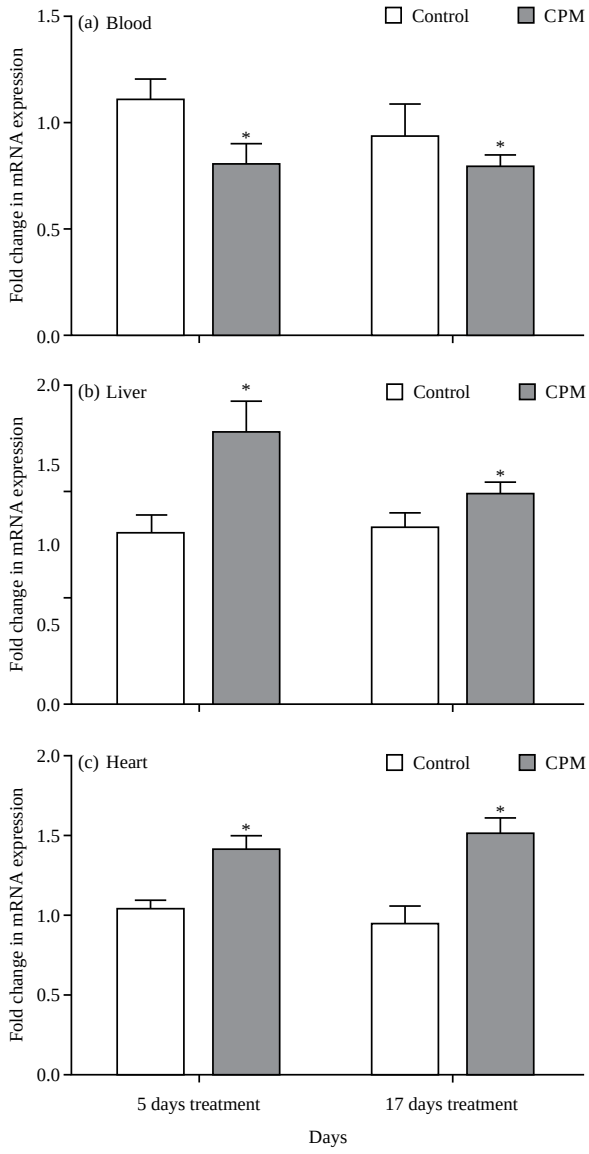

Fig. 8(a-c): Expression levels of *CAT* gene mRNA by RT-PCR semi-quantitative method in the (a) Blood, (b) Liver and (c) Heart samples. CPM-induced toxicity in young male Wistar rats

Values are Mean±SEM (n = 10). *p<0.05, vs. control (one-way analysis of variance (ANOVA) followed by Duncan's test)

different behavioral challenges has been observed and H1-Receptor showed perturbations in sleep-wake cycle[22]. These findings confirm the behavioral results of animal's sleepiness, indolence and inactivity in the present study.

The liver is the center of detoxifying and eliminating the toxic substances that are carried to it through the blood. So, it is uniquely exposed to a wide variety of exogenous and endogenous products, which include environmental chemicals and toxins[23].

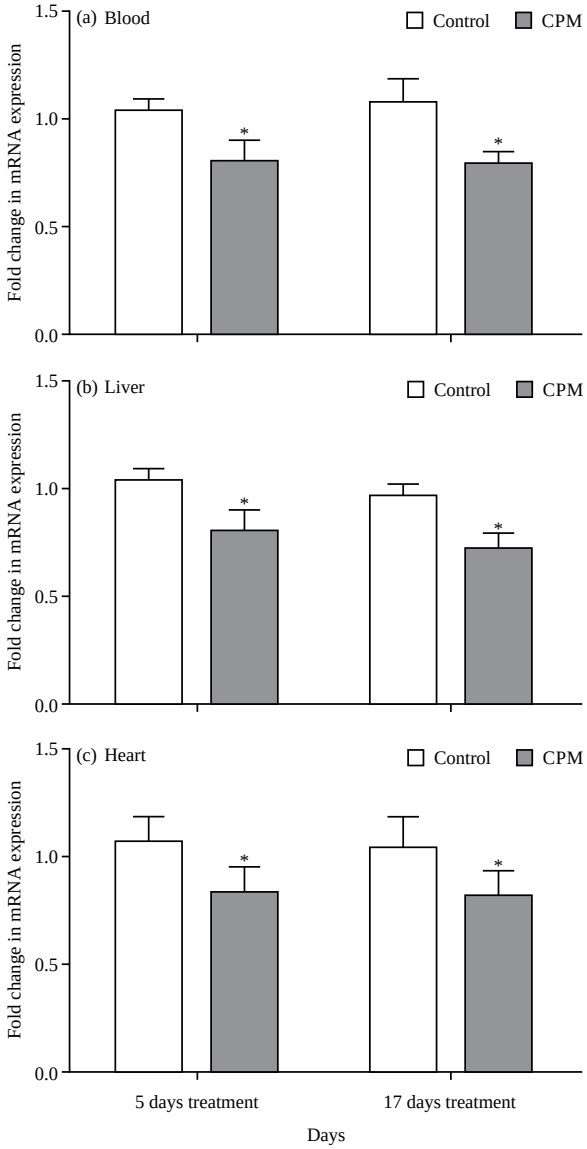

Fig. 9(a-c): Expression levels of *GSHPx* gene mRNA by RT-PCR semi-quantitative method in the (a) Blood, (b) Liver and (c) Heart samples, CPM-induced toxicity in young male Wistar rats

Values are Mean±SEM (n = 10). *p<0.05, vs. control (one-way analysis of variance (ANOVA) followed by Duncan's test)

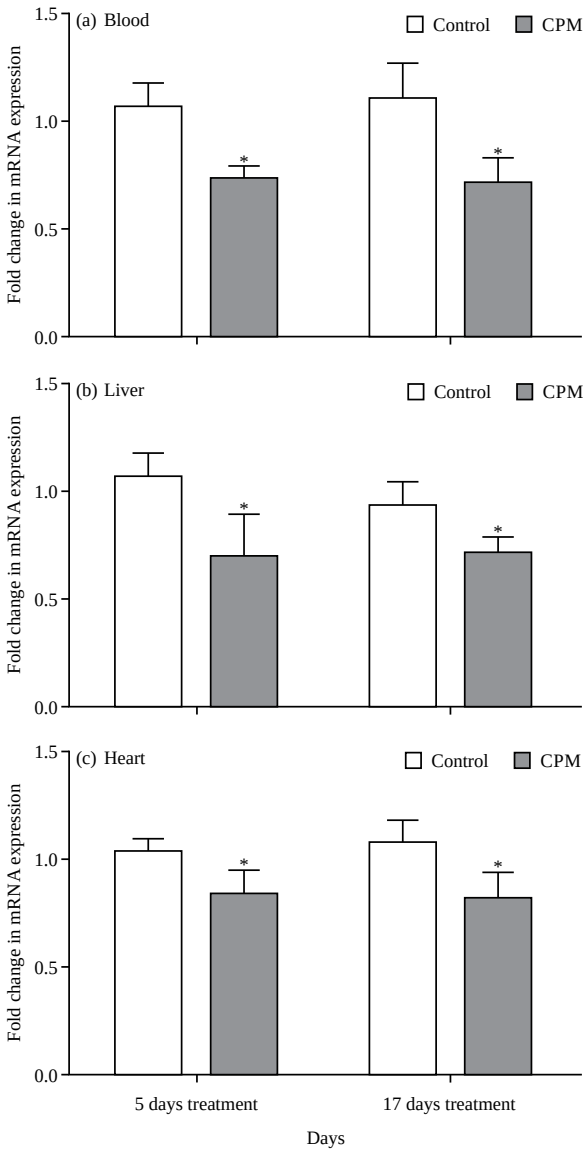

Fig. 10(a-c): Expression levels of *GST* gene mRNA by RT-PCR semi-quantitative method in the (a) Blood, (b) Liver and (c) Heart samples in CPM-induced toxicity in young male Wistar rats

The current results clearly showed that the liver tissues responded markedly to the effect of the antihistamine drug used. The increase of binucleated and hypertrophied hepatocytes was observed in all treated groups particularly GII b, suggesting that mitosis is changed which could be a response to genotoxicity of CPM and to compensate the loss of cells caused by this drug. These findings were consistent with those of OLD Kachi and French[24] and Slott *et al.*[25] who reported that the proportion of binucleated liver cells depends on variables such as regeneration, response to genotoxic or non-genotoxic carcinogens, neoplasia and the importance of hepatocyte hypertrophy in contributing of the development of preneoplastic lesions.

In addition, CPM treated groups showed bile duct proliferation which could play an important role in repairing and rebuilding hepatocytes after CPM administration. These findings are supported by Jack *et al.*[26] who stated that the liver, especially in rats, has a considerable capacity for regeneration, which occurs as surviving hepatocytes undergo mitosis to offset the loss of cells caused by hepatotoxic agents.

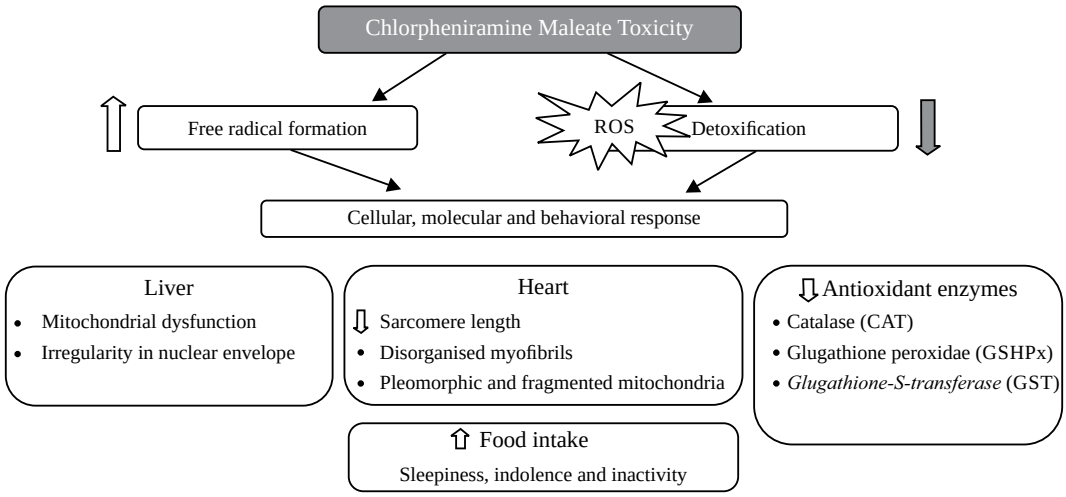

Fig.11: Summary of the CPM main results

CPM administration enhances the free radical generation in the liver and heart of male Wistar rats. This elevation in ROS production may inhibit balance between the oxidant and antioxidant systems. Thus further confirming that free radicals and oxidative damage certainly play a vital role in the pathogenesis of acute liver and heart injury

The mechanisms of regeneration have been suggested to be specific, to some degree and bile duct cellular proliferation aimed to restore the initial number of cells and re-establish hepatic function.

The proliferation of bile duct-like structures is also a hepatic cellular reaction observed in most forms of human liver disease and a variety of experimental conditions associated with liver injury[27]. However, Ghadially[28] stated that biliary lining epithelia of the bile ducts in biliary diseases are known to have intraepithelial atypical/proliferative lesions related to the development of cholangiocarcinoma.

Alterations of nuclei dimensions were observed in hepatocytes of treated animals. Decrease of nuclear size, margination of nuclear heterochromatin and irregularity of nuclear envelope, necrosis and increased number of nucleoli were observed. This observation is similar to that in the case of malignancy[29] and after treatment with drugs as erythromycin[30] and anti-inflammatory drugs[31].

During this study, cellular infiltration in the portal area and hypertrophied nuclei of endothelium within the sinusoids and Kupffer cells, were observed in the liver after administration of CMP in all treated groups. This cellular infiltration of Kupffer cells is considered a sign of chronic inflammation, where these cells phagocyte the causes of damage and damaged tissues[32]. The hypertrophy of these cells may be due to the active defense of these cells in the process of phagocytosis of degenerate red blood cells and the defense against the toxicity and bleeding. Also, the hypertrophied endothelium plays an important role in the inflammatory actions as well[33].

When the endothelium is affected by the infection, stress, hypertension, dyslipidemia, or high homocysteine levels, it undergoes changes resulting in "dysfunction", characterized typically by decreased endothelial expression of nitric oxide, enhanced expression of cell adhesion molecules and associated increased binding of circulating leukocytes to these cells. There are accompanying cytokine and chemokine elaboration, resulting in cellular recruitment and the orchestration of an acute inflammatory response that can culminate in chronic inflammation if reparative mechanisms are not operative[34].

Widened intercellular space between hepatocytes which is due to the expansion of the hepatic portal vein after CPM administration as well as moderate to intense hyalinization of cytoplasmic hepatocytes were observed in the liver of rat in all treated groups. Hyalinization is a group of several degenerative processes that affect various cells and tissues, resulting in the formation of rounded masses (droplets) or relatively broad bands of substances that are homogeneous, translucent, refractile and moderately to deeply acidophilic; may occur as droplets in parenchymal cells[35].

Hawkins *et al.*[36] observed hyalinized hepatocytes after administration of paracetamol at a dose level 500 mg kg^{-1} b.wt., into rats, which caused hepatic toxicity that commonly occurs with acute overdoses and is the foremost cause of liver damage[37]. There is a notable increase in hepatocyte autophagic vacuolation during sepsis; this increase is associated with the mitochondrial injury. It is not possible to justify whether the increase in autophagic vacuolization is due to an adaptive response or a harbinger of cell death[38].

The light microscope of hepatocytes of treated rats, 17 days after administration of CPM (GII b) revealed noticeable cytopathological changes. The most important changes observed were pleomorphic nuclei; that ranged in their degenerative changes from karyolysis to severe karyorrhexis and complete pyknosis. Karyolysis is often described as a late reaction to intoxication in vertebrates and invertebrates[39]. These alterations might be due to the binding of toxins to the chromatin, but can also be related to alterations in membranes or any other metabolic changes leading to cell death.

Concerning cardiac muscles, morphometric results of the present study showed that the sarcomere length significantly decreased after CPM administration as compared to the corresponding control, indicating an alteration in the contractile ability of the heart. This finding is in agreement with Maruyama[40] who showed that the length of sarcomere is the most important parameter of assessing the contractile capacity of any muscle and it is a good indicator of the ability of the muscle to maintain protracted tension.

Terfenadine (H1-receptors blocker) and Astemizole are non-sedating antihistaminics known for inducing torsades de points syndrome, i.e., QT interval prolongation and life-threatening ventricular tachycardia. Each is found to prolong cardiac repolarization when its metabolic elimination is impaired, either by liver disease or drugs that inhibit the 3A family of cytochrome P450. *In vitro* studies indicate that this action is due to blockade of one or more cardiac potassium channels that determine the duration of the action potential[41].

The first generation compounds of antihistamines are known to be competitive inhibitors of muscarinic receptors and cause tachycardia by impairing vagal tone on the heart and xerostomia by inhibiting muscarinic stimulation of salivary function[42].

Washed striation, disorganized myofibrils, irregular or ruptured sarcolemma, were observed in the myocardium of all treated animals with CPM in the current study. All of these changes may lead to loss and degeneration of myofibrils, as described previously by Van *et al.*[43]. Also, the results of the present study are in agreement with Mair and Tomé[44] who stated that the term "myofibrillary degeneration" is used to describe changes affecting myofilaments and Z-lines in myofibers undergoing degeneration and atrophy from various causes. Degeneration and atrophy of myofibers have been observed in a variety of pathological states affecting muscle. These include deprivation of blood supply, metabolic insufficiency, drug action and many other diseases, including muscular dystrophy and myositis.

During this study, the mitochondria increased dramatically in the myocardium of rats treated with CPM. The mechanism whereby CPM inhibition leads to increased cellular mitochondria is unknown. The ultrastructural alterations in mitochondria suggest a decrease in mitochondrial energy production, which is probably an important cause of the nuclear changes previously discussed. Also, these alterations may be due to interactions of the toxin with membrane components and changes in ion transport along the mitochondrial membrane. It is well known that mitochondria are "life-essential" organelles for the production of metabolic energy in the form of ATP and they are generally sensitive to many kinds of stress and react very quickly with gross pathological symptoms, as swelling, shrinkage, disruption of cristae, or formation of intramitochondrial crystals[45]. According to Anttinen *et al.*[46], mitochondrial changes (increase in number) in organophosphate-intoxicated animals are indicative of the increased energy requirements necessary for the cells to overcome the toxic effects of the organophosphorus compound.

The current study showed that mitochondria were aggregated in the form of clumps in the defected cardiac muscle fiber in GII b. This observation agrees with Anttinen *et al.*[46] who stated that the increased number of mitochondria in any pathological condition reflects the process of uncoupling of oxidative phosphorylation. Indeed, several studies showed the relation between mitochondrial damage and drug toxicity.

The activity of various serum biochemical parameters was studied to evaluate the effect of chlorpheniramine maleate on young male Wistar rats in this study. ALT was increased but not statistically significant. However, ALP was increased significantly in treated group GII b compared to the control. This result is in agreement with Ngozika *et al.*[47] who reported that there is an increase of ALT and AST of erythrocyte after administration of the three anti-histamine drugs chlorpheniramine maleate (Piriton), cyproheptadine hydrochloride (Cypron) and clemastine fumarate (Tavegyl) at dose level 0.04, 0.02, 0.01 and 0.005 mg mL^{-1} for 30 days in Wistar albino rats.

Antioxidants reduce the cellular damage resulting from the interaction between lipid, protein and DNA molecules and ROS. Regardless of the presence of this antioxidants system, an over or unbalanced production of the ROS due to contact with chemicals may result in some clinical disorder. The current study investigates the CPM course's hepatotoxicity, cardiotoxicity and hematological toxicity by induction of oxidative stress in the liver, cardiac muscle and blood.

The damage at the cellular level by oxidant is attenuated by antioxidant enzymes such as CAT, GSHPx and GST. CAT and *GSHPx* catalyze the dismutation of the superoxide anion (O^{2-}) into hydrogen peroxide (H_2O_2) which then converts hydrogen peroxide to water, in this manner, protecting against ROS. The CPM decreased the *GSHP* and *GST* activities which were confirmed by the gene expression mRNA expression levels of antioxidant enzymes in the liver and cardiac muscle. These enzymes protect tissues from highly reactive hydroxyl radical (•OH), derived from H_2O_{217}. Results show that CPM administration did not only increase the free radical formation but also decreased its ability to detoxify reactive oxygen species.

CONCLUSION

This study showed that chlorpheniramine maleate (CPM) induced many histological and ultrastructural alterations in cardiac muscle and liver tissue of Wistar rats. In addition, CPM induced a significant decrease in the level of antioxidant genes expression glutathione peroxidase (GSHPx) and glutathione-s-transferase (GST) in blood, liver and heart tissue of rat. Moreover, the level of catalase (*CAT*) gene expression increases significantly in the liver and heart tissues, meanwhile it significantly decreases in blood. Finally, CPM did not increase the free radical formation only but also decreased its ability to detoxify reactive oxygen species.

SIGNIFICANCE STATEMENT

The significance of this study is that it investigated the adverse side effects of the antihistamine chlorpheniramine maleate upon different organs of the Wistar rat for the first time. Based on the current findings, future researchers are advised to investigate the optimal period required for tissue recovery. Future researchers should investigate the genes responsible for producing the new proteins that appeared in the cardiac muscles during treatment and those that disappeared. They are also advised to find the right drug that should be co-administered with CPM to compensate for the alterations in the antioxidant genes and block the oxidative stress pathway.

ACKNOWLEDGMENTS

The authors extend their appreciation to:

- "Research Center of Female Scientific and Medical Colleges", Deanship of Scientific Research, King Saud University
- Deanship of Scientific Research at Princess Nourah Bint Abdulrahman University through the Fast-Track research funding program

REFERENCES

1. Abdel Moneim, A.E., 2016. Indigofera oblongifolia prevents lead acetate-induced hepatotoxicity, oxidative stress, fibrosis and apoptosis in rats. Plos One, 10.1371/journal.pone. 0158965.
2. Al-Shabanah, O.A., M.M. Hafez, M.M. Al-Harbi, Z.K. Hassan, S.S. Al-Rejaie, Y.A. Asiri and M.M. Sayed-Ahmed, 2010. Doxorubicin toxicity can be ameliorated during antioxidant L-carnitine supplementation. Oxid. Med. Cell. Longev., 3: 428-433.
3. Ambree, O., J. Buschert, W. Zhang, V. Arolt, E. Dere and A. Zlomuzica, 2014. Impaired spatial learning and reduced adult hippocampal neurogenesis in histamine H_1-receptor knockout mice Eur. Neuropsychopharmacol., 24: 1394-1404.
4. Anttinen, H., L. Ryhanen, U. Puistola, A. Arranto and A. Oikarinen, 1984. Decrease in liver collagen accumulation in carbon tetrachloride-injured and normal growing rats upon administration of zinc. Gastroenterology, 86: 532-539.
5. Armstrong, R.N., 1991. Glutathione S-transferases: reaction mechanism, structure and function. Chem. Res. Toxicol., 4: 131-140.
6. Baker, A.M., D.G. Johnson, J.A. Levisky, W.L. Hearn, K.A. Moore, B. Levine and S.J. Nelson, 2003. Fatal diphenhydramine intoxication in infants. J. Forensic Sci., 48: 425-428.
7. Dadkhah, A., F. Fatemi, S. Ababzadeh, K. Roshanaei, M. Alipour and B.S. Tabrizi, 2014. Potential preventive role of Iranian *Achillea wilhelmsii* C. Koch essential oils in acetaminophen-induced hepatotoxicity. Bot. Stud., Vol. 55, No. 1.10.1186/ 1999- 3110-55-37.
8. Dixon, L.J., M. Barnes, H. Tang, M.T. Pritchard and L.E. Nagy, 2013. Kupffer cells in the liver. Wiley Online Lib., Vol. 3, No. 2. 10.1002/cphy.c120026.
9. Ebaid, H., M.A. Dkhil, M.A. Danfour, A. Tohamy and M.S. Gabry, 2007. Piroxicam-induced hepatic and renal histopathological changes in mice. Libyan J. Med., 2: 82-89.
10. FDA, 2017. Tussionex pennkinetic extended-release suspension label. https://www.accessdata.fda.gov/drugs atfda_docs/label/2017/019111s019lbl.pdf
11. Fernández, C.D., L. Boscá, L.F. Simón, A. Alvarez and M. Cascales, 1993. Relationship between genomic DNA ploidy and parameters of liver damage during necrosis and regeneration induced by thioacetamide. Hepatol., 18: 912-918.
12. Ghadially, F.N., 1988. Ultrastructural Pathology of the Cell and Matrix: a Text and Atlas of Physiological and Pathological Alterations in the Fine Structure of Cellular and Extracellular Components. 3rd Edn., Elsevier, London; Boston, Butterworths, ISBN: 9781483192086.

13. Glorieux, C. and P.B. Calderon, 2017. Catalase, a remarkable enzyme: targeting the oldest antioxidant enzyme to find a new cancer treatment approach. Biol. Chem., 398: 1095-1108.
14. Goel, A. and D.K. Dhawan, 2001. Zinc supplementation prevents liver injury in chlorpyrifos-treated rats. Biol. Trace. Elem. Res., Vol. 82. 10.1385/BTER:82:1-3:185.
15. Guengerich, F.P., 2011. Mechanisms of drug toxicity and relevance to pharmaceutical development. Drug Metab. Pharmacokinet., 26: 3-14.
16. Hawkins, L.C., J.N. Edwards and P.I. Dargan, 2007. Impact of restricting paracetamol pack sizes on paracetamol poisoning in the united kingdom. Drug Saf., 30: 465-479.
17. Jack, E.M., P. Bentley, F. Bieri, S.F. Muakkassah-Kelly and W. Stäubli *et al*., 1990. Increase in hepatocyte and nuclear volume and decrease in the population of binucleated cells in preneoplastic foci of rat liver: A stereological study using the nucleator method. Hepatol., 11: 286-297.
18. Kachi, K. and S.W. French, 1994. The connection between the nuclei of binucleated hepatocytes: an ultrastructural study. J. Submicrosc. Cytol. Pathol., 26: 163-172.
19. Khashab, M., A.J. Tector and P.Y. Kwo, 2007. Epidemiology of acute liver failure. Curr. Gastroenterol. Rep., 9: 66-73.
20. Liu, H., Q. Zheng and J.M. Farley, 2006. Antimuscarinic actions of antihistamines on the heart. J. Biomed. Sci., 13: 395-401.
21. M. Viluksela, H. Hanhijarvi, R.F.A. Husband, V.M. Kosma, Y. Collan and P.T. Mannisto, 1988. Comparative liver toxicity of various erythromycin derivatives in animals. J. Antimicrob. Chemothe., 21: 9-27.
22. Mair, W.G.P. and F.M.S. Tome, 1972. Atlas of the Ultrastructure of Diseased Human Muscle. Elsevier, Baltimore, Williams and Wilkins, ISBN: 978-0-443-00831-3, Pages: 250.
23. Maruyama, K., 1994. Connectin, an elastic protein of striated muscle. Biophys. Chem., 50: 73-85.
24. Ng, K.H., D. Chong, C.K. Wong, H.T. Ong, C.Y. Lee, B.W. Lee and L.P.C. Shek, 2004. Central nervous system side effects of first- and second-generation antihistamines in school children with perennial allergic rhinitis: a randomized, double-blind, placebo-controlled comparative study. Pediatrics, 113: e116-e121.
25. Ngozika, B.O., C.M. Comfort, A.U. Austin, J.I. Chineye and U.O.Chukwubuike, 2012. Effects of some antihistamine on erythrocyte aspartate amino transferase and alanine amino transferase activities in Wistar albino rats. Indian J. Sci. Technol., 5: 3001-3002.
26. Obrebski, S., 1986. The effects of stress and pollution on marine animals. Q. Rev. Biol., 61: 136-137.
27. Paget, G.E., 1977. Quality assurance in toxicology. Proc. R. Soc. Med., 70: 453-454.
28. Papp, L.V., J. Lu, A. Holmgren and K.K. Khanna, 2007. From selenium to selenoproteins: Synthesis, identity and their role in human health. Antioxidant Redox Signaling, 9: 775-806.
29. Parmentier, R., Y. Zhao, M. Perier, H. Akaoka and M. Lintunen *et al*., 2016. Role of histamine H_1-receptor on behavioral states and wake maintenance during deficiency of a brain activating system: A study using a knockout mouse model. Neuropharmacol., 106: 20-34.
30. Pate, R.R., J.R. O'Neill, W. Byun, K.L. McIver, M. Dowda and W.H. Brown, 2014. Physical activity in preschool children: comparison between montessori and traditional preschools. J. Sch. Health, 84: 716-721.
31. Pawankar, R., G.W. Canonica, S. Holgate, R.F. Lockey and M.S. Blaiss, 2013. The WAO White Book on Allergy. World Allergy Organization, United States of America, ISBN-13: 978-0-615-92915-6.
32. Rajendran, P., T. Rengarajan, J. Thangavel, Y. Nishigaki, D. Sakthisekaran, G. Sethi and I. Nishigaki, 2013. The vascular endothelium and human diseases. Int. J. Biol. Sci., 201: 1057-1069.
33. Sanderson, J., 1999. Biomedical electron microscopy: illustrated methods and interpretations. J. Microsc., 196: 81-82.
34. Simons, F.E.R., 1994. Ancestors of allergy. Global Medical Communications New York, ISBN: 13 9780963938862.
35. Simons, F.E.R., 2002. Comparative pharmacology of H_1antihistamines: clinical relevance. American J. Med., 113: 38-46.
36. Simons, F.E.R., 2004. Advances in H_1-antihistamines. N. Engl. J. Med., 351: 2203-2217.
37. Slott, P.A., M.H. Liu and N. Tavoloni, 1990. Origin, pattern and mechanism of bile duct proliferation following biliary obstruction in the rat. Gastroenterol., 99: 466-477.
38. Storms, W.W., 1997. Treatment of allergic rhinitis: effects of allergic rhinitis and antihistamines on performance. Allergy Asthma proc., 18: 59-61.
39. Suvarna, K., C. Layton and J. Bancroft, 2019. Bancroft's Theory and Practice of Histological Techniques. 8th Edn., Elsevier, US, ISBN: 9780702068645, Pages: 672.
40. Taglialatela, M., H. Timmerman and L. Annunziato, 2000. Cardiotoxic potential and CNS effects of first-generation antihistamines. Trends Pharmacol. Sci., 21: 52-56.
41. Tashiro, M., H. Mochizuki, Y. Sakurada, K. Ishii and K. Oda *et al*., 2006. Brain histamine H_1receptor occupancy of orally administered antihistamines measured by positron emission tomography with^{11}C-doxepin in a placebo-controlled crossover study design in healthy subjects: a comparison of olopatadine and ketotifen. Br. J. Clin. Pharmacol., 61: 16-26.
42. Van Loo, G., X. Saelens, M. van Gurp, M.MacFarlane, S.J. Martin and P. Vandenabeele, 2002. The role of mitochondrial factors in apoptosis: a Russian roulette with more than one bullet. Cell Death Differ., 9: 1031-1042.
43. Von Mutius, E., 2000. The burden of childhood asthma. Arch. Dis. Child., 82: ii2-ii5.

44. Watanabe, E., J.T. Muenzer, W.G. Hawkins, C.G. Davis and D.J. Dixon*et al*., 2009. Sepsis induces extensive autophagic vacuolization in hepatocytes: a clinical and laboratory-based study. Lab. Invest., 89: 549-561.
45. Whalen, K., 2018. Lippincott Illustrated Reviews: Pharmacology. 7th Edn., Lippincott Williams and Wilkins, Philadelphia, ISBN: 9781496384133, Pages: 576.
46. Woosley, R.L., 1996. Cardiac actions of antihistamines. Annu. Rev. Pharmacol. Toxicol., 36: 233-252.
47. Zen, Y., S. Aishima, Y. Ajioka, J. Haratake and M. Kage *et al*., 2005. Proposal of histological criteria for intraepithelial atypical/proliferative biliary epithelial lesions of the bile duct in hepatolithiasis with respect to cholangiocarcinoma: Preliminary report based on interobserver agreement. Pathol. Int., 55: 180-188.